



Dual-pol radar calibration and correction of the bias introduced by non uniform radome wetting

R. Bechini¹, R. Cremonini¹, E. Gorgucci², L. Baldini²

¹ ARPA Piemonte – Area Previsione e Monitoraggio Ambientale, Torino, Italy.

² Institute of Atmospheric Sciences and Climate – CNR, Roma (Italy).

1 Introduction

The increasing interest for polarimetric measurements in operational radar systems requires careful consideration of calibration issues. Arpa Piemonte manages two C-band polarimetric and Doppler radars, located near Torino in Bric della Croce at 0.74 km MSL and near Savona in Monte Settepani over the Apennines at 1.40 km MSL, respectively. Both radar antennas are covered by radome, which is considered an essential protection to guarantee continuous operation during severe weather conditions. The Settepani site, where strong winds often coupled with freezing rain or snow are likely to occur from November to April is particularly critical. Besides periodical electronic calibration, we exploit properties of natural scatterers in order to calibrate ZDR and ZH, using data from the operational volume scans. The self-consistency principle (Gorgucci et al. 1992, Scarchilli et al. 1996) is here considered extensively, not only for absolute radar calibration, but also for estimating the bias introduced by radome wetting. It is found that rain above the radar may cause a highly anisotropic attenuation depending on the wind intensity and direction, which tend to accumulate water preferably on the upwind side of the radome. The effect, especially relevant at the Settepani site at 1.4 km MSL, frequently interested by intense winds, may severely affect reflectivity measurements. Results of radar calibration procedure and azimuth-dependent bias corrections are presented.

2 Radar calibration

A proper calibration of radar measurements is needed for any quantitative application. To this purpose we exploit the properties of natural scatterers in order to calibrate first ZDR and then ZH, using data from the operational volume scans.

2.1 Differential reflectivity

Calibration of ZDR is performed exploiting returns from stratiform light to moderate rain. The best way to perform the ZDR calibration is to point the antenna at 90° elevation angle, collecting data at vertical incidence: the expected ZDR should be 0 dB, since at this angle the raindrop shape is seen as nearly circular (Gorgucci et al., 1999). Unfortunately, in order to eliminate regions of transmitter tube recovery, to select data in the far-field, and considering the height of the radar systems (> 0.7 and ~1.4 km MSL for Bric and Settepani respectively), the first useful bins are often in the bright band or above. Another technique foresees the collection of data at horizontal elevation in drizzling rain, which is thought to be mainly composed by very small and spherical droplets, also producing around 0 dB ZDR (Smyth and Illingworth 1998). We adopt a modified technique, that does not need any additional data than those available from the operational volume scan (-0.1° to 28.5° elevation). We selected vertical profiles of reflectivity and differential reflectivity close to the radar during stratiform rain, with uniform reflectivity along the vertical (standard deviation of ZH < 1.5 dB), using data at elevations 3.0° to 28.5° (the lowest elevations are avoided because more contaminated by ground clutter), providing that the highest elevation is below the bright band. We then average over azimuth and time to obtain a smooth profile of ZDR, which is subsequently compared against theoretical values calculated as follows. After averaging over space and time, the mean Drop Size Distribution (DSD) can be well represented by an exponential form, whose parameter Λ is directly related to

Correspondence to: Renzo Bechini.

r.bechini@arpa.piemonte.it

ZDR (Bringi and Chandrasekar 2001). Given a ZDR value at 0° elevation, geometric computation of the modified eccentricity of the drop allow to derive the backscattering cross sections for horizontal and vertical incident fields at a given elevation angle (Doviak and Zrnic, 1993), from which the modified DSD and the expected ZDR at increasing elevation can be derived.

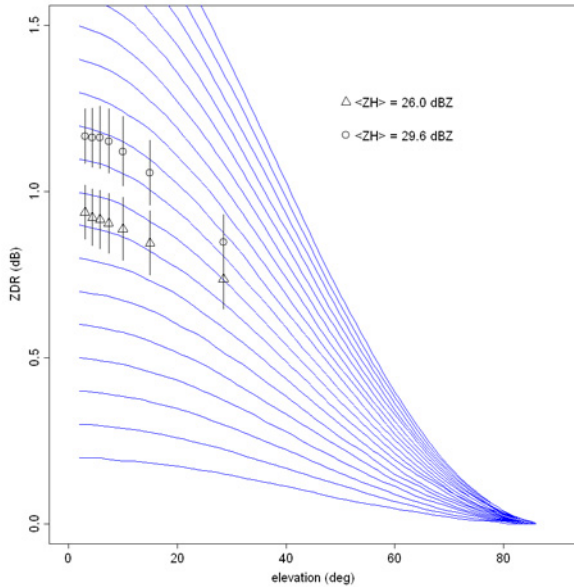


Fig. 1. Average ZDR with error bar given by the standard deviation, over three hours of stratiform precipitation, at operational scan elevation angles for two reflectivity ranges: 20.0-27.5 dBZ (triangles) and 27.5-35.0 dBZ (circles). Theoretical ZDR curves for values at varying view angle starting at 0.2 dB with 0.1 dB increments are overplotted for comparison.

The assessment of the ZDR bias can be finally established finding the value of ΔD which minimizes the RMSE between observed $ZDR + \Delta D$ and theoretical values, that is finding the theoretical ZDR curve which best fit the observed values. Fig. 1 shows theoretical curves with overplotted ZDR average observed values for two reflectivity ranges similarly populated: 20.0-27.5 dBZ and 27.5-35.0 dBZ: the RMSE is minimised for ZDR values giving a bias of respectively 0.9 dB (RMSE = 0.007 dB) and -0.3 dB (RMSE = 0.004 dB), well within the measurement accuracy of ~ 0.2 dB.

Very similar results are obtained for Settepani radar, which showed respectively -0.05 dB and 0.11 dB bias for the two reflectivity ranges. It is concluded that no bias correction is necessary for ZDR on both systems.

2.2 Reflectivity

During the summer of 2005 the Settepani signal processor was upgraded to measure differential propagation phase shift ΦDP and correlation coefficient ρ_{HV} . The availability of ΦDP measurements allowed the application of the self-consistent method for absolute calibration proposed by Gorgucci et al. (1999). Its application will be demonstrated

with the case of September 8, 2005. It was considered to be especially suitable for absolute calibration, due to the presence of widespread light to moderate rain, with high freezing level (3.4 km), nice ΦDP profiles with maximum values beyond 130° and no hail contamination (max ZH \leq 48 dBZ).

The self consistent method relies on theoretical calculations and observational evidence, showing that the three polarization diversity measurements ZH, ZDR and KDP, the specific differential propagation phase shift, given by half the range derivative of ΦDP (Bringi and Chandrasekar 2001), lie in a constrained 3-D space, identified by the following relation:

$$KDP^* = C \cdot Z_H^\alpha \cdot 10^{-\beta \cdot ZDR} \quad (1)$$

where KDP^* is the parameterized estimate of KDP, ZH is in units $mm^6 m^{-3}$ and ZDR is in dB. The values of the coefficients C , α , β at C-band are respectively $1.46 \cdot 10^{-4}$, 0.98, 0.20. In the absence of any system bias a scatterplot of KDP and KDP^* should be about a 1:1 line. The eventual bias on ZH can be estimated by:

$$bias = 10.4 \cdot \log(s) \quad (2)$$

where s is the slope of the scatterplot, while the corresponding standard deviation is given by:

$$\sigma(bias) = 4.52 \cdot \frac{\sigma(s)}{E(s)} \quad (3)$$

where $s(s)$ and $E(s)$ are the standard deviation and mean value of the slope (Gorgucci et al. 1999)

To apply this method, two important pre-processing steps have to be considered:

- 1) filtering of observed ΦDP for KDP calculation.
- 2) attenuation and differential attenuation correction;

Step 1) is accomplished following the iterative procedure proposed by Hubbert and Bringi (1995), with a spatial sampling period of 0.3 km, which attenuates sharply (~ 13 dB) spatial variations of the order of 3 km and less; moreover, in order to work with quantities having the same statistical properties, KDP^* is first integrated in range to calculate ΦDP^* , then both ΦDP and ΦDP^* are filtered using the Hubbert technique, obtaining respectively observed KDP_f and theoretical KDP^*_f , where subscript “f” stands for “filtered” (from now on the subscript will be omitted).

Step 2) is not straightforward, due to the absence of a unique relation for attenuation correction. We used a parameterization of specific attenuation α_H and specific differential attenuation α_D in terms of KDP:

$$\alpha_H = C_H \cdot KDP \quad (4)$$

$$\alpha_D = C_D \cdot KDP \quad (5)$$

Both C_H and C_D are temperature dependent; C_H is also dependent on the drop’s axis ratio, while C_D is much less

sensitive to this parameter, since both αD and KDP are differential quantities (Bringi et al. 2001).

C_D is set to 0.014 (Gorgucci et al. 1998) and the corrected field of ZDR is checked for truthfulness by verification that ZDR values beyond intense precipitation drops to value around 0 dB in regions of low reflectivity (<15 dBZ).

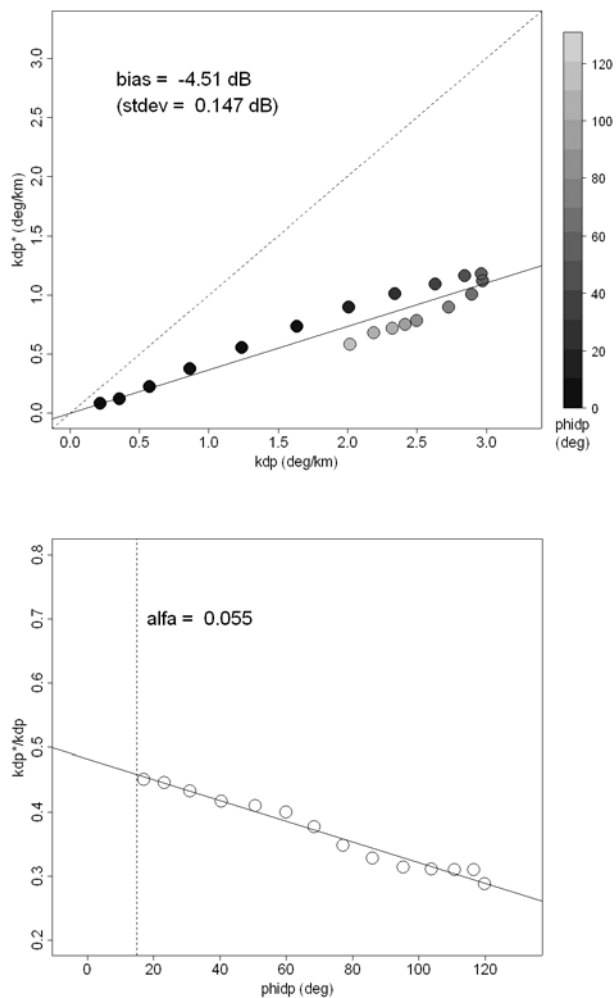


Fig. 2. Scatterplot of KDP* vs. KDP (top) and KDP*/KDP vs. ΦDP (bottom) for $C_H=0.055$, 2005-09-08, 16:40 UTC, elevation = 0.3° , azimuth = 141° .

The value of C_H is first assumed to be 0.055 (Gorgucci et al. 1998) and then it is iteratively adjusted until the slope of the ratio KDP*/KDP versus ΦDP along a radar beam reaches zero. In fact a dependence of the ratio KDP*/KDP with ΦDP , and consequently with total attenuation, indicates that the coefficient C_H assumed is not adequate to represent the specific attenuation along the beam and KDP* is increasingly under or over-estimated with increasing ΦDP .

Fig. 2 and 3 should clarify this procedure: fig 2 (top) shows the scatterplot of KDP* versus KDP with points coloured according to ΦDP and reflectivity data corrected using $C_H=0.055$, for the azimuth 141° at 16:40 UTC, when moderate rain was falling over radome; fig 2 (bottom) shows

the ratio KDP*/KDP versus ΦDP , evidencing a decrease with ΦDP , due to under-corrected attenuation.

Fig. 3 shows the same type of scatterplot, after iteration led to a null slope of KDP*/KDP versus ΦDP for $C_H = 0.082$.

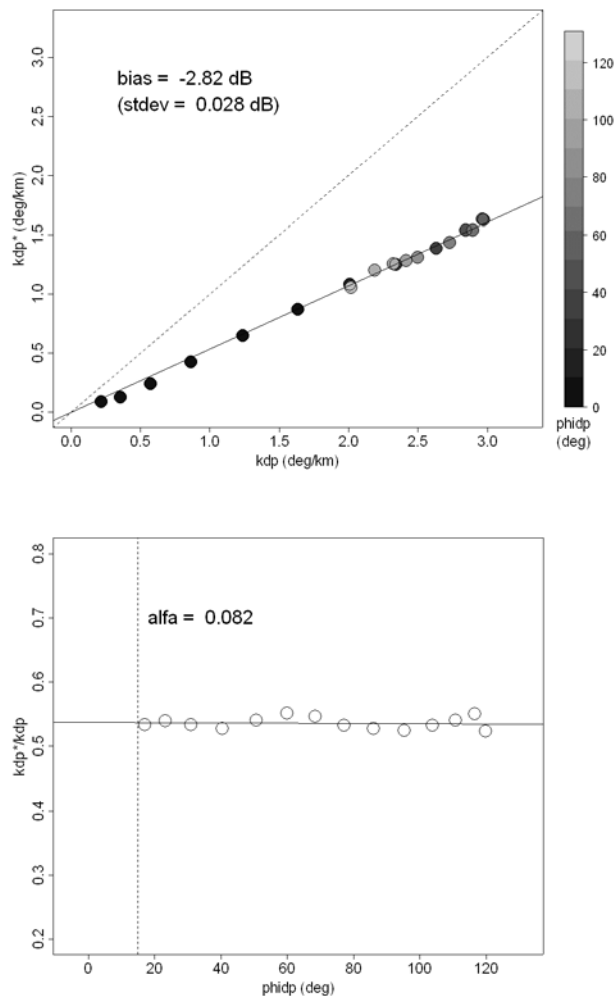


Fig. 3. Same as fig. 2, but for $CH=0.082$, the value of the specific attenuation coefficient which minimizes the slope of KDP*/KDP vs. ΦDP

This adjustment of the attenuation correction coefficient allows a better estimate of the system bias, which for the case shown in fig. 3, is -2.8 dB. Using the standard coefficient C_H would have led to an over-estimation of the absolute value of the bias (-4.5 dB).

The value of C_H have been estimated using radar beams at different azimuth, using data from the lowest three elevations ($-0.3, 0.3, 1.0$ deg) to remain in the rain medium along a path of at least 80 km from the radar, and at different times, corresponding to different rain regimes over radar, with a consequent variety of bias induced by the water load over radome: for a good estimate of the KDP*/KDP versus ΦDP slope, only radar beams reaching high ΦDP values ($>60^\circ$) are considered (a lower threshold at 15° is also applied, to avoid poorly attenuated data). The C_H values found are quite stable and ranges between 0.08 and 0.09 (average 0.085 with

standard deviation 0.004), therefore assuming an intermediate value between 0.055 (reported by Gorgucci et al., 1998, for $T=15^{\circ}\text{C}$) and 0.113 (reported by Testud et al., 2000). Imposing a constant $C_H = 0.085$, the system bias may finally be calculated for every radar beam.

3 Effects of non-uniform radome wetting

Fig. 4 shows the bias estimates as a function of azimuth for two radar scans at 0.3° elevations: solid line with circles represents data at 16:40 UTC, when it was raining over the radar (average reflectivity of 28.2 dBZ around the radar), triangles marks bias estimates at 17:10 UTC when no rain was occurring over the radar (average reflectivity of 11.3 dBZ around the radar). The Doppler velocity at 16:40 UTC near the radar (solid line, right axis) is also shown, to enhance the strong bias dependence (up to ~ 4 dB!) on the wind direction, which is responsible for a differential water load over the radome surface, between downwind (negative Doppler velocity) and upwind (positive Doppler) side.

Fig. 5 summarizes the bias estimation for two radar volume scans, considering the lower three elevations, with no rain over the radome, from which it may be concluded that the system is properly calibrated to within ± 1 dB.

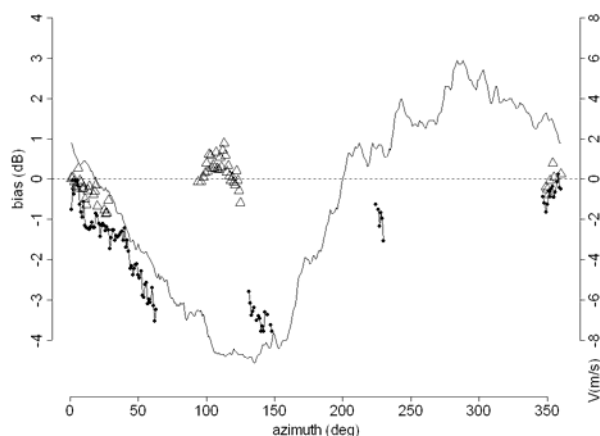


Fig. 4. Bias estimates vs. azimuth for 0.3° elevation at 2005-09-08 16.40 UTC (solid line with circles), with rain over radar, and 17:10 UTC (triangles), no rain over radar. The average Doppler velocity at 16:40 UTC, between 3 and 5 km from the radar, is also shown (solid line, right axis).

4 Conclusions

The results shown lead to consider the added value brought by Φ_{DP} , especially for radar covered by radome. In fact it is commonly acknowledged that for accurate polarimetric measurements a good antenna performance, possibly without any cover, is essential. On the other hand operational radars, to operate in severe weather conditions, often need a radome, which may induce to degrade the polarimetric capabilities of such systems. The reported strong azimuthal dependence of the bias caused by precipitation over the radar can lead up to a factor of two under-estimation of rainfall rate estimated by reflectivity along the most radome-attenuated directions.

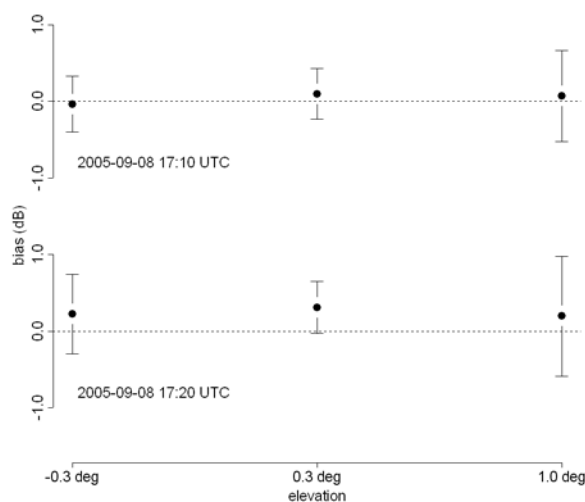


Fig. 5. Bias estimation with error bar for two volume scans (17:10 and 17:20 UTC) at three elevations, in no rain over radar condition.

References

- Bringi, V. N., and V. Chandrasekar, 2001: Polarimetric Doppler Weather Radar: principles and applications. Cambridge University Press, 648 pp.
- Bringi V. N., T. D. Keenan, and V. Chandrasekar, 2001: Correcting C-band radar reflectivity and differential reflectivity data for rain attenuation: A self-consistent method with constraints, *IEEE Trans. Geosci. Remote Sens.*, **39**, 1906–1915.
- Doviak R. and D.S. D. S. Zrić, 1993: Doppler Radar and Weather Observations", Academic Press, , 562 pp.
- Gorgucci, E., G. Scarchilli, and V. Chandrasekar, 1992: Calibration of radars using polarimetric techniques. *IEEE Trans. Geosci. Remote Sens.*, **30**, 853–858.
- Gorgucci, E.; Scarchilli, G.; and V. Chandrasekar, V., 1999: A procedure to calibrate multiparameter weather radar using properties of the rain medium *IEEE Trans. Geosci. Remote Sens.*, **37**, 269 - 276.
- Gorgucci, E., Scarchilli, G., Chandrasekar, V. , Meischner P. F. and M. Hagen, "Intercomparison of techniques to correct for attenuation of C-band weather radar signals," *J. Appl. Meteor.*, **37**, 845–853, 1998.
- Hubbert, J. and V. N. Bringi, 1995: An iterative filtering technique for the analysis of copolar differential phase and dual-frequency radar measurements, *J. Atmos. Ocean Tech.*, **12**, 643-648.
- Scarchilli, G., E. Gorgucci, V. Chandrasekar, and A. Dobaie, 1996: Self-consistency of polarization diversity measurement of rainfall. *IEEE Trans. Geosci. Remote Sensing*, **34**, 22–26.
- Smyth, T. J. and A. J. Illingworth, Correction for attenuation of radar reflectivity using polarization data, 1998: *Quart. J. Roy. Meteor. Soc.*, **124**, 2393-2415.
- Testud, J, Le Bouar E., Obligis E., and M. Ali-Mehenni, 2000: The rain profiling algorithm applied to polarimetric weather radar, *J. Atmos. Oceanic Technol.*, **17**, 332–356.